Addy, J. W. G., Ellis, R. H., MacLaren, C., Macdonald, A. J., Semenov, M. A. and Mead, A. 2022. A heteroskedastic model of park grass spring hay yields in response to weather suggests continuing yield decline with climate change in future decades. *Journal of the Royal Society Interface.* 19, p. 20220361. https://doi.org/10.1098/rsif.2022.0361

A Heteroskedastic Model of Park Grass Spring Hay Yields in Response to Weather Suggests Continuing Yield Decline with Climate Change in Future Decades

John W. G. Addy, Richard H. Ellis, Chloe MacLaren
Andy J. Macdonald, Mikhail A. Semenov, Andrew Mead

August 18, 2022

Abstract

UK grasslands perform important environmental and economic functions, but their future productivity under climate change is uncertain. Spring hay yields from 1902 to 2016 at one site (the Park Grass Long Term Experiment) in southern England under four different fertiliser regimes were modelled in response to weather (seasonal temperature and rainfall). The modelling approach applied comprised: (1) a Bayesian model comparison to model parametrically the heteroskedasticity in a Gamma likelihood function; (2) a Bayesian varying intercept multiple regression model with an autoregressive lag one process (to incorporate the effect of productivity in the previous year) of the response of hay yield to weather from 1902 to 2016. The model confirmed that warmer and drier years, specifically, autumn, winter and spring, in the 20th and 21st centuries reduced yield. The model was applied to forecast future spring hay yields at Park Grass under different climate change scenarios (HadGEM2 and GISS RCP 4.5 and 8.5). This application indicated that yields are forecast to decline further between 2020 and 2080, by as much as 48-50%. These projections are specific to Park Grass, but implied a severe reduction in grassland productivity in southern England with climate change during the 21st century.

1 Introduction

Grassland ecosystems perform critical environmental and economic roles. In the UK, grassland covers nearly 40% of the total land area (Morton 2021), supporting a wide range of biodiversity (Boatman et al. 2007) and providing important ecosystem services such as carbon storage (Ward et al. 2016, Alonso et al. 2021) and rainfall capture to reduce flooding (ONS 2018). Managed grassland (rough grazing and pasture) is the UK's largest crop by area at over 12 million hectares (DEFRA 2021), and underpins a livestock sector worth over 13 billion GBP each year.

With global mean temperatures already 1.43°C above the 20th century average (NOAA 2017) and predicted to increase to at least 1.5°C above the 20th century average by the end of the 21st century (Pörtner et al. 2022), it is vital to understand the impact of climate change on UK grasslands. In general, anthropogenic climate change is detrimental to ecosystems (Runting et al. 2017, Pörtner et al. 2022). The rapid rate of change is exceeding the abilities of many organisms to adapt or migrate, resulting in widespread deterioration in ecosystem structure and function (Pörtner et al. 2022). Grasslands, however, may be less negatively affected than other ecosystems, with Gao et al. (2016) observing either apparent increases or no changes in global grassland productivity between 1982 and 2011, and Hufkens et al. (2016) predicting an increase in productivity for North American grasslands under future climate scenarios.

The impacts of climate change are however site specific, and not all grasslands are responding positively. Wu et al. (2021) have observed consistent productivity declines in across all major grassland types in northern China, while Brookshire & Weaver (2015) documented a >50% decline in a grassland in the Greater Yellowstone Ecosystem in the USA. In the UK, Qi et al. (2018) predict an overall slight decline (2.5-5%) in the productivity of permanent grasslands, but emphasise that differences in local weather patterns resulting from climate change are likely to lead to different outcomes in different locations.

In this study, we seek to increase understanding of climate change impacts on UK grassland productivity using 114 years of data (1902-2016) from the Park Grass Experiment. We use these data to parameterise a model linking hay yield to temperature and precipitation. The modelling approach applied comprised: (1) a Bayesian model comparison to model parametrically the heteroskedasticity in a Gamma likelihood function, which compared three

methods for modelling heteroskedasticity; (2) a Bayesian varying intercept multiple regression model with an autoregressive lag one process (to incorporate the effect of productivity in the previous year) of the response of hay yield to weather (rainfall and temperature) from 1902 to 2016, using the parametric structure of the mean-variance relationship assessed in (1). We then forecast annual productivity under different climate scenarios and models from 2020 to 2080.

2 Materials

2.1 Long-Term Hay Yield Data

The Park Grass Experiment is an agricultural and ecological long-term experiment which has investigated the effects of inorganic fertilisers and organic manures on permanent grassland since 1856 (Lawes & Gilbert 1859). It is thought to be the oldest experiment on permanent grassland in the world. Early on it became clear that the treatments affected species com- position dramatically from what had been a uniform sward comprising about 50 species (Lawes & Gilbert 1880, 1859). The continuing effects on species diversity and on soil function of the original treatments, together with later tests of liming and interactions with atmospheric inputs and climate change, has made Park Grass increasingly important to ecologists, environmentalists, and soil scientists (Silvertown et al. 2006). Studies of the variability of grassland yield have concluded that the use of fertilisers (especially nitrogen) have led to the dominance of grasses on some of the plots on Park Grass (Silvertown et al. 1994, Köhler et al. 2012, Macdonald et al. 2018) and that hay yields are affected by productivity in the previous year (Jenkinson et al. 1994, Kettlewell et al. 2006, Silvertown et al. 1994). Historically, the rainfall from March to July has been shown to be positively related to grassland production (Cashen 1947, Lawes & Gilbert 1880). More recently, warmer temperatures have been shown to be negatively associated with hay yield (Addy et al. 2021).

Recent research has examined how long-term agricultural field experiments can improve our understanding of current scientific issues, such as the effects of changes in the management in soil organic matter (Poulton et al. 2018), and how changes in weather influence the yields of winter wheat given different amounts of nitrogen fertilizer (Addy et al. 2020). Studies into understanding variations in grassland yield have concluded that the use of fertilisers (especially nitrogen) have led to the dominance of grasses on some of

the plots on Park Grass (Silvertown et al. 1994, Köhler et al. 2012, Macdonald et al. 2018). Further research has also shown a dependence in hay yield productivity with the previous year (Jenkinson et al. 1994, Kettlewell et al. 2006, Silvertown et al. 1994).

We developed our modelling approach of the Park Grass hay yield data by incorporating an understanding of the predictive distribution of this dataset into the model. The variances of hay yields from the plots on Park Grass experiment increase as total yields increase, illustrating non-constant residual variances, also known as heteroskedastic errors. Heteroskedastic errors are common for yield data, which can lead to biased estimates of model coefficients (Damesa et al. 2018). Non-constant residual variances may be modelled as a functional response of model predictions (Carroll & Ruppert 1988). Such models include replacing the mean-variance relationship with a known relationship such as a quadratic function (Argyropoulos et al. 2017). We show here how the parametric log-logistic function can be used to model heteroscedastic errors of the Gamma likelihood function for Park Gras hay yields (harvested around mid-June) from 1902 to 2016. The dependence of hay yield productivity with the previous year is formalised by including an autoregressive lag-one term in our model. We then apply our model to forecast spring hay yields until 2080 under different future climate scenarios.

The Park Grass Long-Term Experiment comprises of several different fertiliser regimes. Treatments were selected to provide a range of four fertiliser regimes, to assess whether climate impacts differed between nutrient-limited grassland (typical of natural grasslands) and nutrient-rich grassland (typical of grassland managed for forage or biomass production). Yields from the longest time-series plots (unlimed treatments) were selected as they provide the longest time-series. The treatments selected were no fertiliser (plots 2.2, 3, 12), 96 kg N ha^{-1} plus minerals (P, K, Na & Mg; plot 14.2), 48 kg N ha^{-1} plus minerals (plot 16) and minerals only (plot 7). Plots 14.2 and 16 both received N as sodium nitrate; P, K, Na and Mg were applied as triple superphosphate (17 kg P ha^{-1}), potassium sulphate (225 kg K ha^{-1}), sodium sulphate (15 kg Na ha^{-1}) and magnesium sulphate (10 kg Mg ha^{-1}) respectively. Here we present an analysis of the hay yields (harvested around mid-June) from 1902 to 2016. A change in harvest method was introduced in 1960; yields from 1960 onwards were corrected using the relationship derived by Bowley et al. (2017) to facilitate a continuous analysis of hay yields over the selected time periods. For more information about these plots and the Park Grass experiment more generally see Macdonald et al. (2018).

2.2 Rothamsted Meteorological Station Data

Seasonal total rainfall (TR; mm of rainfall per 3 months) and mean temperature (MT; [daily maximum temperature °C + daily minimum temperature °C]/2 averaged over three months) from 1902 to 2016 were derived from the Rothamsted Meteorological Station records. The cropping season for these analyses were from autumn to spring (September – May inclusive) each year.

The mean annual temperature at Rothamsted (UK) has been steadily increasing from the 1970s to 2016, with slight year-to-year variability (Figure 1 & Supplementary Figure 1). Compared to mean temperature, there has been no trend in annual total rainfall from 1902 to 2016, only considerable year-to-year variability (Figure 1).

2.3 Future Climate Scenarios

Transient climate scenarios for the period 2017 to 2080 were generated by the LARS-WG stochastic generator (Lazzarotto et al. 2010, Semenov et al. 2010, Semenov & Stratonovitch 2015) and were based on the climate projections from global climate models (GCMs) from the Coupled Model Intercomparison Project Phase 5 (CMIP5) ensemble (Taylor et al. 2012). To account for uncertainty in future climate projections two contrasting GCMs from the CMIP5 ensemble were used, i.e. HadGEM2-ES from the UK Meteorological Office (Martin et al. 2011) and GISS-E2-R-CC from the Goddard Institute for Space Studies (Chandler et al. 2013). Predicted absolute changes in mean annual temperature over Northern Europe by 2080 for the RCP 8.5 emission scenario (Moss et al. 2010) were substantially different for these two GCMs, 6.1 °C for HadGEM2-ES (Figure 1) compared to 3.9 °C for GISS-E2-R-CC (Supplementary Figure 1)(Semenov & Stratonovitch 2015). The CMIP5 simulations were driven by a set of emission scenarios consistent with the Representative Concentration Pathways (RCPs) (Moss et al. 2010). The four RCPs were based on a range of projections of future population growth, technological development and societal responses, i.e. RCP 8.5 (business-as-usual or a worst-case emission scenario), RCP6.0 (stabilisation without overshoot), RCP 4.5 (stabilisation without overshoot) and RCP2.6 (peak and decline). To account for uncertainty resulting from emission scenarios, we used two RCPs, i.e. RCP 4.5 and RCP 8.5. For each combination of GCM and RCP, LARS-WG was applied to generate 1000 transient samples which were used as inputs to the statistical models to forecast future spring hay yields.

3 Modelling the Predictive Density

3.1 Constant Variance and heteroskedasticity

In this section we investigate how changing the variance function can improve the predictive accuracy of a model fitted to the Park Grass hay dataset. For the four different fertiliser treatments (six plots in total) the variance in hay yield increases as yields increase. We compare the use of several methods (Table 1) and compare the predictive accuracy of each method in a Bayesian model comparison (Figure 2).

We can predict hay yield y_i (t dm ha^{-1}) as a linear combination of variables (x_{ij}) and model parameters β_j (e.g. mean spring temperature °C) such that, $y = X\beta + \varepsilon$. Where, y is the vector of observed hay yields from 1902 to 2016, X is the matrix of model variates of interest, β_j is a list of j model coefficients and ε is the error term of the model, with model predictions $\hat{y}$ being estimated as $X\beta$. Assuming $y_i \sim N(X\beta, \sigma^2)$, where the model variance σ^2 is constant over all predictions $\hat{y}_i$, we may obtain the probability of observation i given model parameters β and variance σ^2 ($p(y_i|\beta, \sigma^2)$). One issue with this commonly-used model form is the assumption $y_i \sim N(X\beta, \sigma^2)$ is the one of constant variance over all observations of y. We observe heteroskedasticity of hay yield (Supplementary Figure 2), where variability in hay yields increases with higher yields. As shown in Supplementary Figure 2, a Normal likelihood function with constant variance (Model 1, see Table 1) was fitted to the Park Grass hay yield data to illustrate the impacts of heteroskedasticity. This model over-predicted the variance at low yields and under-predicted at higher yields, with credible intervals going into the negative for smaller yields.

There are several ways to deal with non-constant residual variance of a continuous response variable, as seen for hay yields here. A common method involves the transformation of the response variable, y, using either the square-root or natural-log function (Welham et al. 2014), depending on the severity of non-constant residual variance. For the square-root transformation the distribution of the model is now given as $p(\sqrt{y}|\beta, \sigma^2)$, with all inferences about model coefficients and model error given on the scale of $\sqrt{y}$. Model 2 in Supplementary Figure 2 shows that a Normal model with constant variance on the square-root scale adequately modelled the variation in hay yield of the Park Grass experiment across the range of plots. Although the variances seem low, all inferences about model coefficients and model error are given on the scale of $\sqrt{y}$ and predictions have to be back-transformed onto the original scale of the data.

Heteroskedasticity of model residuals may also be modelled using a Gamma likelihood function for data which is non-negative, such as these hay yields. From a Gamma likelihood function, $y_i \sim Gamma(\upsilon, \lambda_i)$ with a shape parameter υ and separate rate parameter λ for each prediction ($\hat{y}_i$). For non-negative values in y, a log-link function, $\log(y) = X\beta$, may be used to ensure the prediction of positive values (Dobson 1990). The Gamma likelihood function for hay yield (y) is given as $p(y|\upsilon, \lambda)$ and can be reparameterised to incorporate model predictions of y, with $\hat{y} = e^{X\beta}$, given $\hat{y} = \upsilon/\lambda$ and $\sigma^2 = \hat{y}^2/\upsilon$ (McCullagh & Nelder 1989).

Model 3 in Supplementary Figure 2 shows the fitted Gamma model to Park Grass hay yield data. The variance around yields from low-yielding plots (plots 3, 2.2, 12) was adequately modelled, but was drastically over-estimated for higher-yielding plots (plots 16 and 14.2). We may decide to model each plot (j) with their own shape parameter (υ_j). A model with individual shape parameters for each plot adequately estimated the variance at low and high yields. However, such an approach fails to model the mean-variance relationship of Park Grass hay yields as part of the underlying biological process and this relationship may be better understood as a function of model predictions.

3.2 Modelling Variances

The variance associated with Park Grass hay yields was shown to vary with predictions of y that could not be modelled adequately with a common shape parameter from a Gamma distribution. The mean-variance relationship may be modelled with an estimate of σ_i^2 for each $\hat{y}_i$. Where, $\text{var}(y) = g(\hat{y}|\tau)$ (Carroll & Ruppert 1988) with τ variance parameters. Although heteroskedasticity may be modelled by shape parameter υ of the Gamma likelihood function, the mean-variance relationship of the Park Grass dataset was shown to plateau with mean estimates greater than 3 t ha^{-1} (see Model 4 as illustrated in Supplementary Figure 2). We may use a non-parametric smooth relationship for a mean-variance relationship (Muller & Stadtmuller 1987). However, we can use a three parameter non-linear log-logistic functional relationship,

$$\text{var}(y) = \tau_3 \Big/ \left(1 + e^{(-(\hat{y}-\tau_1)/\tau_2)}\right) \tag{1}$$

(Finney 1971), where, τ_1 is the mid-point in the log-logistic curve, τ_2 the rate towards the mid-point and τ_3 the maximum variance for a mean prediction. The likelihood function is now conditional on model parameters β and variance parameters τ ($p(y|\beta, \tau)$). The fitted mean-variance relationship is given

in Supplementary Figure 2 as Model 5, where the variances around each plot were adequately modelled using a three parameter log-logistic function (Equation 1) and have similar estimates as Model 4.

3.3 Bayesian Priors and Posteriors

Given the likelihood function of the Normal distribution, posterior densities of model coefficients may be derived through Bayes rule, where

$$p(\beta, \sigma^2|y) \propto p(y|\beta, \sigma^2)p(\beta)p(\sigma^2)$$

(Gelman et al. 2013, Lee 2012). A Cauchy(25) prior (Gelman 2006) was used for σ^2 for both models Model 1 and Model 2. For Model 3 and Model 4, a uniform prior was used for the shape parameter for the Gamma likelihood. Priors for the variance log-logistic model, Model 5, were empirically chosen through investigation of the model parameters. The posterior for Model 5 becomes,

$$p(\beta, \tau|y) \propto p(y|\beta, \tau)p(\beta)p(\tau).$$

For posterior estimates above, samples were drawn from a gradient based Hamiltonian Markov Chain (Neal 2010). The Hamiltonian Markov Chain was written in R (R Core Team 2018), with 2000 iterations used to sample the model posterior with a burn-in of 100 samples. For all analyses, 89% credible intervals were used, see McElreath (2020) for information regarding credible region.

3.4 Model Prediction

The posterior predictive distribution of all models fitted was obtained by

$$p(\tilde{y}|y) = \int p(\tilde{y}|\theta^*)p(\theta^*|y)d\theta^*$$

(Gelman et al. 2013). The value θ represents a list of model and variance coefficients β and τ (or σ^2 depending on the model), $\tilde{y}$ the new simulated data, and θ^* the sampled coefficients from the Markov Chain. One thousand samples were drawn randomly from the model posterior, $p(\theta^*|y)$, and simulated predictions were based on the given likelihood functions (McElreath 2020).

3.5 WAIC and Selecting Predictive Distribution

We have already discussed the fitting adequacy of each of the models described in Table 1. We used the Watanabe–Akaike Information Criterion

(WAIC) (Watanabe 2013, 2010) to compare the predictive accuracy (Vehtari et al. 2017) of the Normal and Gamma models outlined above. The WAIC was preferred over such summaries as the coefficient of determination to understand the predictive accuracy of the proposed variance models as the WAIC incorporates variance structures through the likelihood function. For all WAIC values, 89% Bootstrapped credible intervals were calculated for Models 1, 3, 4 and 5 (McElreath 2020). Model comparison of the WAIC could not be achieved for Model 2, due to inferences not being conducted on the natural scale of the data.

3.6 Posterior Predictive Accuracy

When comparing the overall model fits, Models 4 and 5 had the lowest WAIC values (Figure 2), and so the best predictive accuracy. The WAIC for the Normal model with constant variance (Model 1) and for the Gamma model with a constant shape parameter (Model 3) had the highest WAIC values and therefore had the poorest predictive accuracy. Modelling the mean-variance relationship of the Gamma model as a log-logistic function (Model 5) provided a similar model fit to a Gamma model with individual shape terms for each plot (Model 4). Model 5 was preferred over Model 4 as we modelled the functional mean-variance relationship of hay yields. Although Model 4 gives a similar predictive fit to Model 5, when modelling covariates, such as weather, a functional understanding of the mean-variance relationship was preferred.

3.7 Modelling Covariates

Having addressed the issue of heteroskedasticity of model errors and by functionally modelling the mean-variance relationship as a three parameter log-logistic function (Model 5) to better understand the predictive distribution of the Gamma likelihood, we investigated the influence of weather on the historic Park Grass hay yields. Hay yield was modelled as a linear combination of weather variables and a lag-one autoregressive process (β_ρ) (Marin & Robert 2014), with varying intercepts for each treatment (β_j; $j = 2.2$, 3, 12, 14.2, 16 and 7). The lag-one autoregressive process accounts for the correlation of the previous year's yield with the current year's yield. The relationship between spring rainfall and temperature and hay yield was curvilinear and modelled as a quadratic relationship (i.e. each of rainfall and temperature represented by linear and quadratic terms). (A log-link function was used to model parameters, and therefore model parameters refer to the link scale.)

The autoregressive lag-one process, β_ρ was modelled as $\log(y_{t-1_i})$ to be on the same scale as the log-link function.

4 Hay Yield and Climate Change

4.1 Influence of Covariates on Hay Yields

From the model presented here, warmer temperatures in autumn and winter were negatively associated with subsequent hay yields on Park Grass, $\beta_{\text{MTAut (deg C)}} = -0.045$ (SD= 0.004) and $\beta_{\text{MTWin (deg C)}} = -0.013$ (SD = 0.006) (Table 2). With average seasonal temperatures steadily increasing at Rothamsted from 1902 to 2016 (Figure 1) and hay yields from the Park Grass Experiment steadily declining over the same period, this association supports the evidence that warmer temperatures tend to reduce yield in grasslands (Addy et al. 2021). The effect of each weather variable in spring (both rainfall and mean temperature) was curvilinear, with negative coefficients for the second order quadratic terms (Table 2), suggesting an optimum spring weather to maximise spring hay yields. The relative magnitude of decline in hay yields due to an increase in autumn mean temperature was considerably greater than for winter mean temperature. However, due to the curvilinear relationship between hay yield and mean spring temperature, the effect of increase in spring temperature was dependent upon whether or not the optimum temperature was transgressed and if so by how much (Supplementary Figure 9). If spring temperature increases much further in future then hay yield loss will become yet more severe.

From our model (Table 2), the autoregressive lag-one estimate was estimated as $\beta_\rho = 0.304$ (SD = 0.019). Hence any benefit from good weather for hay yield in year $t-1$ has a carryover to hay yield in year t. Due to the log-link function to guarantee positive estimates of hay yield, an increase of 1 in log yield at year $t-1$ would increase predicted yield in year t by 35% (1–exp(0.304)). Auto-regressive processes for the yield of perennial crops are often overlooked but are important to include to maximise the predictive accuracy of models (and for some crops, autoregressive processes may extend over several years). Although an autoregressive lag p process of the Park Grass dataset may have been modelled, a lag-one process was selected because this process is well documented in Park Grass hay yields (Jenkinson et al. 1994, Kettlewell et al. 2006, Silvertown et al. 1994).

4.2 Modelling Variances

Modelling the mean-variance relationship of the Gamma likelihood for hay yields as a log-logistic function was successful in overcoming the over-estimation of variances seen for the earlier models (Figure 4). The variance associated with hay yield increased up to a yield of around 2-3 t ha^{-1}, after which the variance associated with yield plateaued (Figure 4), with a maximum estimated variance of 0.731 (SD = 0.041) (Table 2; τ_3 parameter see Equation 1).

The success of this modelling approach shows how variances may be modelled by functions sampled from a posterior distribution. However, the use of a parametric function to model the mean-variance relationship may be considered as another assumption of the model, and other functions may be needed to model the mean-variance relationship in other datasets. The log-logistic function was chosen because the variances of Park Grass hay yields were shown to plateau at mean estimates greater than 3 t ha^{-1} (see Model 4 in Supplementary Figure 2).

4.3 Hay Yield in Future Climate Scenarios

Using the HadGEM2 weather model, forecasted hay yields to 2080 under RCP 4.5 and 8.5 showed decreasing hay production across all plots (Figure 3). RCP 4.5 and 8.5 gave similar predictions for yield until 2060, after which RCP 8.5 projections continued to decline while RCP 4.5 plateaued. The high-input plots 14.2 and 16 of the Park Grass experiment had the greatest absolute decline in hay yield across all future climate projections. However, all plots had a relative decline of around 50% (Table 3). In 1902 the projected hay yield for section 14.2 was 4.24 t ha^{-1} (CI: 2.92, 5.77; Figure 3), in 2080 for HadGEM2 RCP 8.5 the forecast hay yield for plot 14.2 is 2.01 t ha^{-1} (CI: 0.97, 3.65), 47.51% lower than the respective 2020 yields (Table 3). Generally, using HadGEM2 weather model (Figure 2) forecast a steeper decline in annual yield compared to forecasts based on the GISS climate model (Supplementary Figure 3, Supplementary Table 1). The projections for hay yield under GISS RCP 4.5 declined until 2060 and plateaued thereafter, whereas those under GISS RCP 8.5 continued to decline between 2060 and 2080 (by an average of 25.2% across all plots).

5 Discussion

From 1902 to 2016, there were associations between (a) warmer autumn and winter temperatures and lower hay yields and (b) spring rainfall and hay

yields in all four contrasting fertiliser regimes (six plots) at Park Grass (Table 2). (For a visual summary of the covariates from the Park Grass weather varying intercept model see Supplementary Figures 4-9.) These responses concur with previous studies which showed the yield of grassland to be reduced by warmer temperatures (Addy et al. 2021) and less rainfall (Cashen 1947, Lawes & Gilbert 1880). Further, there was a forecast decline of hay yields from 2020 to 2080 for RCP 8.5 for both HadGEM2 and GISS across all future climate scenarios, with climate model HadGEM2 providing a greater relative decline in hay yield compared to GISS. This forecasted decline in hay yields was due to warmer temperatures which are expected to rise throughout the 21st century for both HadGEM2 and GISS (Figure 1 & Supplementary Figure 2), as the Park Grass hay model in Table 2 has parameterised the negative relationship between warmer temperatures and lower yields from 1902 to 2016, whilst those models provide no consistent trend in total rainfall from 2020 to 2080.

Excluding rough grazing, over 10 million hectares of grassland are farmed in the UK (DEFRA 2021). Temperate grasslands may be classed by management intensity (Whitehead 2000): intensive, single-species swards for milk producers with high mineral nitrogen application 250-400 kg N year^{-1} (i.e., $>$ plot 14.2); moderate, grass-clover swards with moderate fertiliser inputs (similar to or $<$ plot 16); or extensive, with no inputs (as with plots 2.2, 3, 12). The average mineral nitrogen application on UK grassland was 54 kg ha^{-1} in 2019 (DEFRA 2021). Hence, the results from plot 16, and to a lesser extent 14.2, provide the closest approximation for the impacts of climate change on grassland productivity, at least for southern England. Mean productivity declines of around 20-30% by 2060 are predicted for both climate scenarios, increasing to nearly 50% under RCP 8.5 (Table 3). Such a decline would be expected to have a substantial impact on the livestock sector in the region, requiring farmers to reduce stocking levels, import additional feed from elsewhere, or switch from grass to other forage silages (e.g., forage maize, *Zea mays* L.). The continued retreat of intensive milk production from the region, as intensive grassland productivity declines (Plot 14.2, Figure 3), to wetter and cooler regions of the UK may be a consequence. Hence the results from plot 16, and to a lesser extent 14.2, provide the closest approximation for the impacts of climate change on grassland productivity for southern England in terms of current agronomy; but such comparisons will be affected by variation in soils across the region.

Productivity declines in grassland also have implications for ecosystem service provision. The amount of carbon sequestered in the soil is dependent

on productivity (Jones & Donnelly 2004), and the role of grasslands in flood risk reduction are to some extent dependent on their soil carbon content and associated capacity of the soil to absorb water (Feger & Hawtree 2013). In regard to biodiversity support, the consequences of reduced productivity are more complicated. Plant species diversity typically has a unimodal relationship with productivity; in unproductive systems, both species diversity and productivity tend to be low due to low resource availability or high stress, while in highly productive systems, diversity also tends to be low because low stress and high resource availability favour a few highly productive species that outcompete others (Silvertown et al. 1994, Brun et al. 2019). Therefore, the productivity declines forecast in this paper could be associated with either an increase or decrease in diversity: if climate change reduces productivity via suppressing dominant species, then grassland plant diversity may increase, whereas if climate change reduces productivity via increasing stress for all plant species, or species that are already less prolific, then diversity may decline. Future research looking at how community composition responds to warmer winter temperatures would help to clarify whether climate change is likely to increase or decrease grassland plant diversity. Declines in productivity, with or without changes in plant diversity, will also impact arthropod communities (Prather & Kaspari 2019, Fernández-Tizón et al. 2020) and other taxa (Marriott et al. 2009). Our study of above-ground production provides no information on what is happening beneath the soil surface. Some species within the sward may divert biomass to the roots when plants are under stress. Hence the direct implications of the current results for ecosystem service provision deserve further study, as do the indirect implications of, for example, changes in land use from grassland to other crops.

This study forecasts greater declines of grassland productivity than have been previously predicted for the UK (Thornley & Cannell 1997, Qi et al. 2018). To some extent this is likely to be due to the different scales of studies; our forecasts are for a single site on a single soil type, albeit with a wide range of fertiliser inputs and soil pH (Johnston et al. 1986), while Qi et al. (2018) estimated productivity across the whole of the UK. Weather patterns predicted under future climate scenarios vary spatially across the UK, and different grasslands may respond in different ways. There are also other differences in our models; both Thornley & Cannell (1997) and Qi et al. (2018) included an effect of CO_2 fertilisation, based on observed increases in perennial ryegrass (*Lolium perenne* L.) productivity under higher CO_2. However, we did not include an effect of CO_2 fertilisation due to the monotonic increase in CO_2 from 1902. Grasslands are composed of many more species than ryegrass that may all respond differently, and there is no

evidence that rising atmospheric CO_2 has increased Park Grass hay yields so far (Jenkinson et al. 1994). It has also been concluded that grassland from Park Grass achieved saturation of atmospheric carbon more than one century ago (Baca Cabrera et al. 2021). Furthermore, CO_2 fertilisation effects tend to be negated by increasing temperatures (Ainsworth et al. 2020). It is likely therefore that assuming an effect of CO_2 fertilisation would overestimate grassland productivity under future projections of climate scenarios.

Our study also presents a more robust estimate of the relationship between hay yields and weather variation than previous studies, given our long-term dataset (114 years), our inclusion of an auto-regressive function for hay yields, and our novel approach to modelling the heteroskedasticity of Park Grass hay yields. The autoregressive function reinforces the effect of warming in reducing hay yield because a decline in yield from warming in year $t-1$ also reduces hay yield in year t. Traditional modelling approaches were shown to be restricted by the functional relationship of the mean-variance relationship. Although a non-parametric function may have been used to model the mean-variance relationship of a Normal distribution (Muller & Stadtmuller 1987, Rice & Silverman 1991) we concluded that the functional variance of Park Grass hay yields may be successfully modelled using a three-parameter log-logistic function of the Gamma distribution for non-negative data. However, the variance in yield for the no input (plots 2.2 and 3) and minerals only (plot 7) treatments seem to have low variance around the 1970s. This suggests time-specific variation, but investigation of such a model is beyond the scope of this study. The posterior predictive distribution of Park Grass hay yields and forecasted yields was greatly improved when the mean-variance relationship of a Gamma likelihood function was replaced, which gave similar predictive accuracy to a Gamma model with individual shape parameters for each plot.

Overall, the dramatic grassland productivity declines estimated by this study are a cause for serious concern, emphasising the need to mitigate climate change to sustain grassland farming in the region. Declines in grassland productivity by 2080 of up to 27% under RCP 4.5 and 50% under RCP 8.5 would substantially undermine livestock production in southern England and may also reduce the contributions of grassland to carbon sequestration, flood mitigation, and biodiversity support. It may be possible to monitor future grassland productivity at high spatial-temporal resolution from satellites. However, such monitoring may only be limited to early-21st images and not the 20th comparisons made in this study. To understand whether the predicted declines on the Park Grass Experiment are representative of

grasslands across the UK more widely, future research should explore the response of different grasslands to climate change using models that appropriately account for heteroskedastic variance and autoregressive yields.

Acknowledgements

We thank Margaret Glendining, Sarah Perryman and Tony Scott for access to yield and weather data from the Electronic Rothamsted Archive (e-RA), and the Lawes Agricultural Trust for supporting the work of JWGA as part of a PhD Scholarship. A special thanks is given to the Rothamsted Statistics and Data Science Department for their informative comments. The Rothamsted Library & Information Services are thanked for access to their large collection of historical Rothamsted publications.

The Rothamsted Long-Term Experiments National Capability (LTE-NCG) is supported by the UK Biotechnology and Biological Science Research Council (BBS/E/C/000J0300) and the Lawes Agricultural Trust.

References

Addy, J. W., Ellis, R. H., Macdonald, A. J., Semenov, M. A. & Mead, A. (2020), 'Investigating the effects of inter-annual weather variation (1968–2016) on the functional response of cereal grain yield to applied nitrogen, using data from the Rothamsted Long-Term Experiments', *Agricultural and Forest Meteorology* **284**, 107898.

Addy, J. W., Ellis, R. H., Macdonald, A. J., Semenov, M. A. & Mead, A. (2021), 'Changes in agricultural climate in South-Eastern England from 1892 to 2016 and differences in cereal and permanent grassland yield', *Agricultural and Forest Meteorology* **308**, 108560.

Ainsworth, E., Lemonnier, P. & Wedow, J. (2020), 'The influence of rising tropospheric carbon dioxide and ozone on plant productivity', *Plant Biology* **22**, 5–11.

Alonso, I., Gregg, R., Elias, J., Crosher, I., Muto, P. & Morecroft, M. (2021), 'Carbon storage and sequestration by habitat: a review of the evidence (second edition) Natural England Research Report NERR094. Natural England, York.'.

Argyropoulos, C., Etheridge, A., Sakhanenko, N. & Galas, D. (2017), 'Modeling bias and variation in the stochastic processes of small RNA sequencing', *Nucleic Acids Research* **45**(11), e104–e104.

Baca Cabrera, J. C., Hirl, R. T., Schäufele, R., Macdonald, A. & Schnyder, H. (2021), 'Stomatal conductance limited the CO2 response of grassland in the last century', *BMC Biology* **19**(1), 50.

Boatman, N. D., Parry, H. R., Bishop, J. D. & Cuthbertson, A. G. (2007), 'Impacts of agricultural change on farmland biodiversity in the uk', *Issues in Environmental Science and Technology. No. 25. Biodiversity Under Threat* pp. 1–32.

Bowley, H. E., Mathers, A. W., Young, S. D., MacDonald, A. J., Ander, E. L., Watts, M. J., Zhao, F. J., McGrath, S., Crout, N. & Bailey, E. H. (2017), 'Historical trends in iodine and selenium in soil and herbage at the Park Grass Experiment, Rothamsted Research, UK', *Soil Use and Management* **33**(2), 252–262.

Brookshire, E. & Weaver, T. (2015), 'Long-term decline in grassland productivity driven by increasing dryness', *Nature Communications* **6**(1), 1–7.

Brun, P., Zimmermann, N. E., Graham, C. H., Lavergne, S., Pellissier, L., Münkemüller, T. & Thuiller, W. (2019), 'The productivity-biodiversity relationship varies across diversity dimensions', *Nature Communications* **10**(1), 1–11.

Carroll, R. J. & Ruppert, D. (1988), *Transformation and Weighting in Regression*, Vol. 30, CRC Press.

Cashen, R. O. (1947), 'The influence of rainfall on the yield and botanical composition of permanent grass at Rothamsted', *Journal of Agricultural Science* **37**, 1–9.

Chandler, M., Sohl, L., Jonas, J., Dowsett, H. & Kelley, M. (2013), 'Simulations of the mid-pliocene warm period using two versions of the nasa/giss modele2-r coupled model', *Geoscientific Model Development* **6**(2), 517–531.

Damesa, T. M., Möhring, J., Forkman, J. & Piepho, H.-P. (2018), 'Modeling spatially correlated and heteroscedastic errors in ethiopian maize trials', *Crop Science* **58**(4), 1575–1586.

DEFRA (2021), 'Agriculture in the United Kingdom 2020'.
URL: *www.gov.uk/government/statistics/agriculture-in-the-united-kingdom-2020*

Dobson, A. J. (1990), *An Introduction to Generalized Linear Models*, Chapman & Hall.

Feger, K.-H. & Hawtree, D. (2013), Soil carbon and water security, *in* 'Ecosystem services and carbon sequestration in the biosphere', Springer, pp. 79–99.

Fernández-Tizón, M., Emmenegger, T., Perner, J. & Hahn, S. (2020), 'Arthropod biomass increase in spring correlates with NDVI in grassland habitat', *The Science of Nature* **107**(5), 1–7.

Finney, D. J. (1971), *Probit Analysis: a statistical treatment of the sigmoid response curve*, Cambridge University Press, Cambridge.

Gao, Q., Zhu, W., Schwartz, M. W., Ganjurjav, H., Wan, Y., Qin, X., Ma, X., Williamson, M. A. & Li, Y. (2016), 'Climatic change controls productivity variation in global grasslands', *Scientific Reports* **6**(1), 1–10.

Gelman, A. (2006), 'Prior distributions for variance parameters in hierarchical models', *Bayesian Analysis* **1**(3), 515–534.

Gelman, A., Carlin, J. B., Stern, H. S., Dunson, D. B., Vehtari, A. & Rubin, D. B. (2013), *Bayesian Data Analysis*, CRC press.

Hufkens, K., Keenan, T. F., Flanagan, L. B., Scott, R. L., Bernacchi, C. J., Joo, E., Brunsell, N. A., Verfaillie, J. & Richardson, A. D. (2016), 'Productivity of north american grasslands is increased under future climate scenarios despite rising aridity', *Nature Climate Change* **6**(7), 710–714.

Jenkinson, D. S., Potts, J. M., Perry, J. N., Barnett, V., Coleman, K. & Johnston, A. E. (1994), 'Trends in herbage yields over the last century on the Rothamsted Long-term Continuous Hay Experiment', *The Journal of Agricultural Science* **122**(3), 365–374.

Johnston, A., Goulding, K. & Poulton, P. (1986), 'Soil acidification during more than 100 years under permanent grassland and woodland at rothamsted', *Soil Use and Management* **2**(1), 3–10.

Jones, M. B. & Donnelly, A. (2004), 'Carbon sequestration in temperate grassland ecosystems and the influence of management, climate and elevated CO_2', *New Phytologist* **164**(3), 423–439.

Kettlewell, P., Easey, J., Stephenson, D. & Poulton, P. (2006), 'Soil moisture mediates association between the winter North Atlantic Oscillation and

summer growth in the Park Grass Experiment', *Proceedings of the Royal Society B: Biological Sciences* **273**(1590), 1149–1154.

Köhler, I. H., Macdonald, A. & Schnyder, H. (2012), 'Nutrient supply enhanced the increase in intrinsic water-use efficiency of a temperate semi-natural grassland in the last century', *Global Change Biology* **18**(11), 3367–3376.

Lawes, J. B. & Gilbert, J. H. (1859), 'Report of experiments with different manures on permanent meadow land Part I Produce of hay per acre', *Journal of the Royal Agricultural Society of England* **19**(1), 552–573.

Lawes, J. B. & Gilbert, J. H. (1880), 'Agricultural, botanical and chemical results of experiments on mixed herbage of permanent meadow, conducted for more than 20 years in succession on the same land. Part 1. The agricultural results', *Philosophical Transactions of the Royal Society* **171**, 289–415.

Lazzarotto, P., Calanca, P., Semenov, M. & Fuhrer, J. (2010), 'Transient responses to increasing CO_2 and climate change in an unfertilized grass–clover sward', *Climate Research* **41**(3), 221–232.

Lee, P. M. (2012), *Bayesian Statistics: an Introduction*, John Wiley & Sons.

Macdonald, A. J., Poulton, P., Clark, I., Scott, T., Glendining, M., Perryman, S., Storkey, J., Bell, J., Shield, I., Mcmillan, V. & Hawkins, J. (2018), *Guide to the Classical and other Long-term experiments, Datasets and Sample Archive*, Rothamsted Research.

Marin, J.-M. & Robert, C. P. (2014), *Bayesian Essentials with R*, Springer.

Marriott, C., Hood, K., Fisher, J. & Pakeman, R. (2009), 'Long-term impacts of extensive grazing and abandonment on the species composition, richness, diversity and productivity of agricultural grassland', *Agriculture, Ecosystems & Environment* **134**(3-4), 190–200.

Martin, G., Bellouin, N., Collins, W., Culverwell, I., Halloran, P., Hardiman, S., Hinton, T., Jones, C., McDonald, R., McLaren, A., O'Connor, F. et al. (2011), 'The hadgem2 family of met office unified model climate configurations', *Geoscientific Model Development* **4**(3), 723–757.

McCullagh, P. & Nelder, J. A. (1989), *Generalized Linear Models*, Vol. 37, CRC Press.

McElreath, R. (2020), *Statistical Rethinking: A Bayesian course with examples in R and Stan*, CRC press.

Morton, R.D.;Marston, C. A. C. (2021), 'Land Cover Map 2020 (10m classified pixels, GB)'.

Moss, R. H., Edmonds, J. A., Hibbard, K. A., Manning, M. R., Rose, S. K., Van Vuuren, D. P., Carter, T. R., Emori, S., Kainuma, M., Kram, T. et al. (2010), 'The next generation of scenarios for climate change research and assessment', *Nature* **463**(7282), 747–756.

Muller, H.-G. & Stadtmuller, U. (1987), 'Estimation of heteroscedasticity in regression analysis', *The Annals of Statistics* pp. 610–625.

Neal, R. M. (2010), MCMC using Hamiltonian Dynamics, *in* S. Brooks, A. Gelman, G. Jones & X. L. Meng, eds, 'Handbook of Markov Chain Monte Carlo', Chapman & Hall.

NOAA (2017), 'Global Climate Report - Annual 2016.'.
URL: *https://www.ncdc.noaa.gov/sotc/global/201613*

ONS (2018), 'UK natural capital: developing semi-natural grassland ecosystem accounts.'.
URL: *https://tinyurl.com/2d35zrm5*

Pörtner, H. O., Roberts, D. C., Adams, H., Adler, C., Aldunce, P., Ali, E., Begum, R. A., Betts, R., Kerr, R. B., Biesbroek, R. et al. (2022), *IPCC, 2022: Summary for Policy makers.*

Poulton, P., Johnston, J., Macdonald, A., White, R. & Powlson, D. (2018), 'Major limitations to achieving "4 per 1000" increases in soil organic carbon stock in temperate regions: Evidence from long-term experiments at Rothamsted Research, United Kingdom', *Global Change Biology* **24**(6), 2563–2584.

Prather, R. M. & Kaspari, M. (2019), 'Plants regulate grassland arthropod communities through biomass, quality, and habitat heterogeneity', *Ecosphere* **10**(10), e02909.

Qi, A., Holland, R. A., Taylor, G. & Richter, G. M. (2018), 'Grassland futures in great britain–productivity assessment and scenarios for land use change opportunities', *Science of the Total Environment* **634**, 1108–1118.

R Core Team (2018), *R: A Language and Environment for Statistical Computing*, R Foundation for Statistical Computing, Vienna, Austria.
URL: *https://www.R-project.org/*

Rice, J. A. & Silverman, B. W. (1991), 'Estimating the mean and covariance structure nonparametrically when the data are curves', *Journal of the Royal Statistical Society: Series B (Methodological)* **53**(1), 233–243.

Runting, R. K., Bryan, B. A., Dee, L. E., Maseyk, F. J., Mandle, L., Hamel, P., Wilson, K. A., Yetka, K., Possingham, H. P. & Rhodes, J. R. (2017), 'Incorporating climate change into ecosystem service assessments and decisions: a review', *Global Change Biology* **23**(1), 28–41.

Semenov, M. A. & Stratonovitch, P. (2015), 'Adapting wheat ideotypes for climate change: accounting for uncertainties in cmip5 climate projections', *Climate Research* **65**, 123–139.

Semenov, M., Donatelli, M., Stratonovitch, P., Chatzidaki, E. & Baruth, B. (2010), 'Elpis: a dataset of local-scale daily climate scenarios for europe', *Climate Research* **44**(1), 3–15.

Silvertown, J., Dodd, M. E., McConway, K., Potts, J. & Crawley, M. (1994), 'Rainfall, biomass variation, and community composition in the Park Grass Experiment', *Ecology* **75**(8), 2430.

Silvertown, J., Poulton, P., Johnston, E., Edwards, G., Heard, M. & Biss, P. M. (2006), 'The park grass experiment 1856–2006: its contribution to ecology', *Journal of Ecology* **94**(4), 801–814.

Taylor, K. E., Stouffer, R. J. & Meehl, G. A. (2012), 'An overview of cmip5 and the experiment design', *Bulletin of the American Meteorological Society* **93**(4), 485–498.

Thornley, J. & Cannell, M. (1997), 'Temperate grassland responses to climate change: an analysis using the hurley pasture model', *Annals of Botany* **80**(2), 205–221.

Vehtari, A., Gelman, A. & Gabry, J. (2017), 'Practical Bayesian model evaluation using leave-one-out cross-validation and WAIC', *Statistics and Computing* **27**(5), 1413–1432.

Ward, S. E., Smart, S. M., Quirk, H., Tallowin, J. R., Mortimer, S. R., Shiel, R. S., Wilby, A. & Bardgett, R. D. (2016), 'Legacy effects of grassland management on soil carbon to depth', *Global Change Biology* **22**(8), 2929–2938.

Watanabe, S. (2010), 'Asymptotic equivalence of Bayes cross validation and widely applicable information criterion in singular learning theory.', *Journal of Machine Learning Research* **11**(12).

Watanabe, S. (2013), 'A widely applicable Bayesian information criterion', *Journal of Machine Learning Research* **14**(Mar), 867–897.

Welham, S. J., Gezan, S. A., Clark, S. J. & Mead, A. (2014), *Statistical Methods in Biology: design and analysis of experiments and regression*, CRC Press.

Whitehead, D. C. (2000), *Nutrient elements in grassland: soil-plant-animal relationships*, C.

Wu, G.-L., Cheng, Z., Alatalo, J. M., Zhao, J. & Liu, Y. (2021), 'Climate warming consistently reduces grassland ecosystem productivity', *Earth's Future* **9**(6), e2020EF001837.

Tables

Table 1: Description of each model fitted to hay yields (t ha^{-1} at 100% dry matter) from Park Grass plots 2.2, 3, 12, 14.2, 16 and 7 from 1902 to 2016 to assess the predictive distribution of the data.

Model	Summary
Model 1	Normal model with constant variance. No method of dealing with heteroskedasticity.
Model 2	Normal model with constant variance on the square-root scale of the data. Inferences conducted on the square-root scale of the data.
Model 3	Gamma model with constant shape term.
Model 4	Individual Gamma model for each plot (2.2, 3, 12, 14.2, 16 and 7), with separate shape terms.
Model 5	Gamma model where the variance has been modelled as a log-logistic function of the mean estimate (Equation 1).

Table 2: Parameter estimates, standard deviations, and 89% credible interval of the Park Grass weather varying intercept model using variance model given in Equation 1 and Model 5 from Table 1. This model quantifies the response from 1902 to 2016 of spring (first cut) hay yield (t dm ha^{-1}) in six plots (2.2, 3, 12, 14.2, 16, 7) under different fertilizer regimes to seasonal temperature (MTAut, MTWin, MTSpr) and rainfall (TRAut, TRWin, TRSpr). Terms $_1$ and $_2$ refer to first and second order terms of a quadratic relationship. All β coefficients refer to Park Grass hay yields via the log-link function. See Supplementary Figures 4-9 for the visual summary of the covariates from the Park Grass weather varying intercept model.

Parameter	Coefficient	SD	5.5% CI	94.5% CI
$\beta_{2.2}$	0.472	0.037	0.415	0.534
β_3	0.362	0.039	0.300	0.423
β_{12}	0.512	0.038	0.451	0.574
$\beta_{14.2}$	1.532	0.036	1.472	1.588
β_{16}	1.331	0.033	1.279	1.384
β_7	1.087	0.033	1.035	1.140
β_ρ	0.304	0.019	0.273	0.334
$\beta_{\text{TRAut (mm)}}$	1.772×10^{-6}	1.111×10^{-4}	-1.815×10^{-4}	1.753×10^{-4}
$\beta_{\text{TRWin (mm)}}$	1.285×10^{-5}	1.267×10^{-4}	-1.882×10^{-4}	2.114×10^{-4}
$\beta_{\text{TRSpr}_1\text{(mm)}}$	0.451	0.171	0.175	0.719
$\beta_{\text{TRSpr}_2(\text{mm}^2)}$	-2.475	0.214	-2.824	-2.135
$\beta_{\text{MTAut (deg C)}}$	-0.045	0.004	-0.051	-0.039
$\beta_{\text{MTWin (deg C)}}$	-0.013	0.006	-0.022	-0.004
$\beta_{\text{MTSpr}_1\text{(deg C)}}$	0.187	0.188	-0.119	0.474
$\beta_{\text{MTSpr}_2(\text{deg C}^2)}$	-0.673	0.181	-0.949	-0.375
τ_1	1.256	0.075	1.377	1.137
τ_2	0.464	0.054	0.379	0.552
τ_3	0.731	0.041	0.668	0.798

Table 3: Changes in spring hay yields (t ha^{-1} at 100% dry matter, with 89% credible interval) forecast for Park Grass plots 2.2, 3, 12, 14.2, 16 and 7 in 2020, 2040, 2060, and 2080 from the model given in Table 2 under HadGEM2 RCP 4.5 and 8.5 future climate scenarios. Values Δ % are the percentage change from 2020

Treatment	Year	RCP 4.5	Δ%	RCP 8.5	Δ%
No Input	2020	0.822 (0.262, 1.750)		0.790 (0.260, 1.731)	
(2.2)	2040	0.739 (0.227, 1.692)	-10.136	0.673 (0.219, 1.532)	-14.775
	2060	0.608 (0.183, 1.424)	-26.079	0.524 (0.149, 1.376)	-33.733
	2080	0.620 (0.177, 1.514)	-24.507	0.396 (0.075, 1.030)	-49.903
No Input	2020	0.690 (0.231, 1.617)		0.653 (0.210, 1.493)	
(3)	2040	0.597 (0.192, 1.437)	-13.408	0.567 (0.162, 1.399)	-13.142
	2060	0.528 (0.118, 1.351)	-23.431	0.484 (0.119, 1.289)	-25.950
	2080	0.500 (0.116, 1.273)	-27.584	0.326 (0.050, 0.977)	-50.090
No Input	2020	0.827 (0.275, 1.799)		0.813 (0.278, 1.883)	
(12)	2040	0.794 (0.273, 1.720)	-3.955	0.732 (0.244, 1.668)	-10.037
	2060	0.640 (0.192, 1.482)	-22.538	0.596 (0.165, 1.429)	-26.763
	2080	0.649 (0.184, 1.536)	-21.487	0.414 (0.086, 1.102)	-49.070
96 kg N ha^{-1}	2020	3.926 (2.462, 5.648)		3.838 (2.505, 5.566)	
+ Minerals	2040	3.745 (2.326, 5.322)	-4.590	3.507 (2.106, 5.140)	-8.611
(14.2)	2060	3.103 (1.846, 4.665)	-20.945	2.783 (1.548, 4.216)	-27.493
	2080	3.049 (1.806, 4.680)	-22.340	2.014 (0.965, 3.647)	-47.516
48 kg N ha^{-1}	2020	2.944 (1.731, 4.468)		2.928 (1.774, 4.518)	
+ Minerals	2040	2.685 (1.521, 4.098)	-8.779	2.534 (1.390, 4.132)	-13.463
(16)	2060	2.212 (1.069, 3.833)	-24.870	2.050 (1.001, 3.590)	-29.991
	2080	2.261 (1.128, 3.739)	-23.198	1.492 (0.645, 2.943)	-49.061
Minerals	2020	2.013 (1.017, 3.605)		2.008 (1.016, 3.646)	
(7)	2040	1.838 (0.905, 3.418)	-8.718	1.765 (0.778, 3.268)	-12.081
	2060	1.557 (0.652, 2.894)	-22.674	1.371 (0.555, 2.734)	-31.710
	2080	1.578 (0.663, 3.136)	-21.617	1.029 (0.398, 2.145)	-48.780

Figures

Figure 1: Rothamsted Meteorological Station's harvest season (Autumn to Summer) yearly summary of mean temperature (deg C) and total rainfall (mm) from 1902 to 2016 (blue), with HadGEM2 RCP 4.5 (orange) and 8.5 (red) transient future climate projections from 2017 to 2080 with 89% credible interval (shaded area)

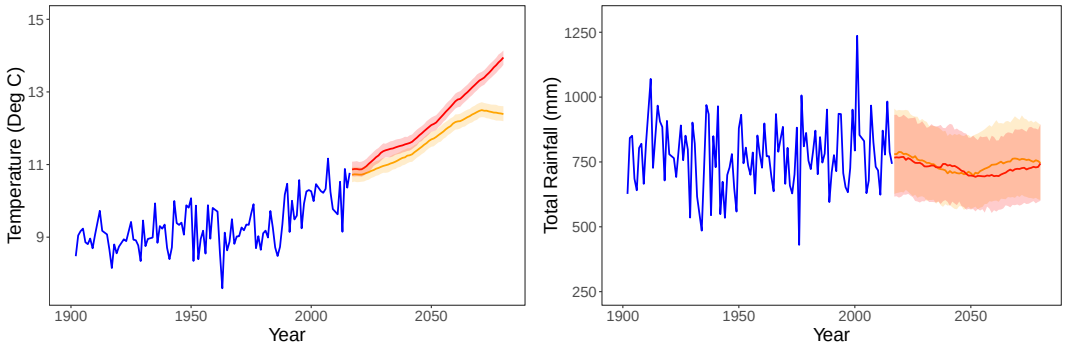

Figure 2: The Watanabe–Akaike Information Criterion (WAIC, •) for Models 1, 3-5 (Table 1) with Bootstrapped 89% credible intervals (shaded area)

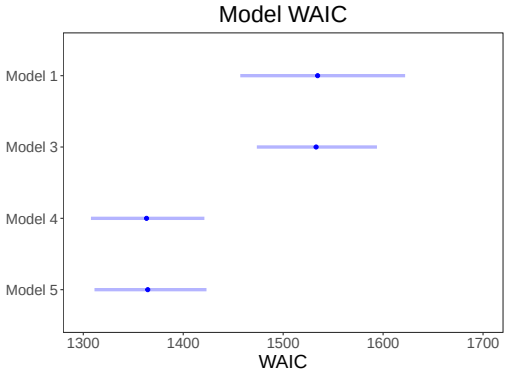

Figure 3: Hay yields (t dm ha^{-1}) from Park Grass plots 2.2, 3, 12, 14.2, 16 and 7 from 1902 to 2016 (•) with forecasted hay yields from HadGEM2 RCP 4.5 (orange) and 8.5 (red) future climate scenarios. Fitted line is the posterior predictive values from the varying intercept Park Grass weather model given in Table 2 with 89% credible interval (shaded area)

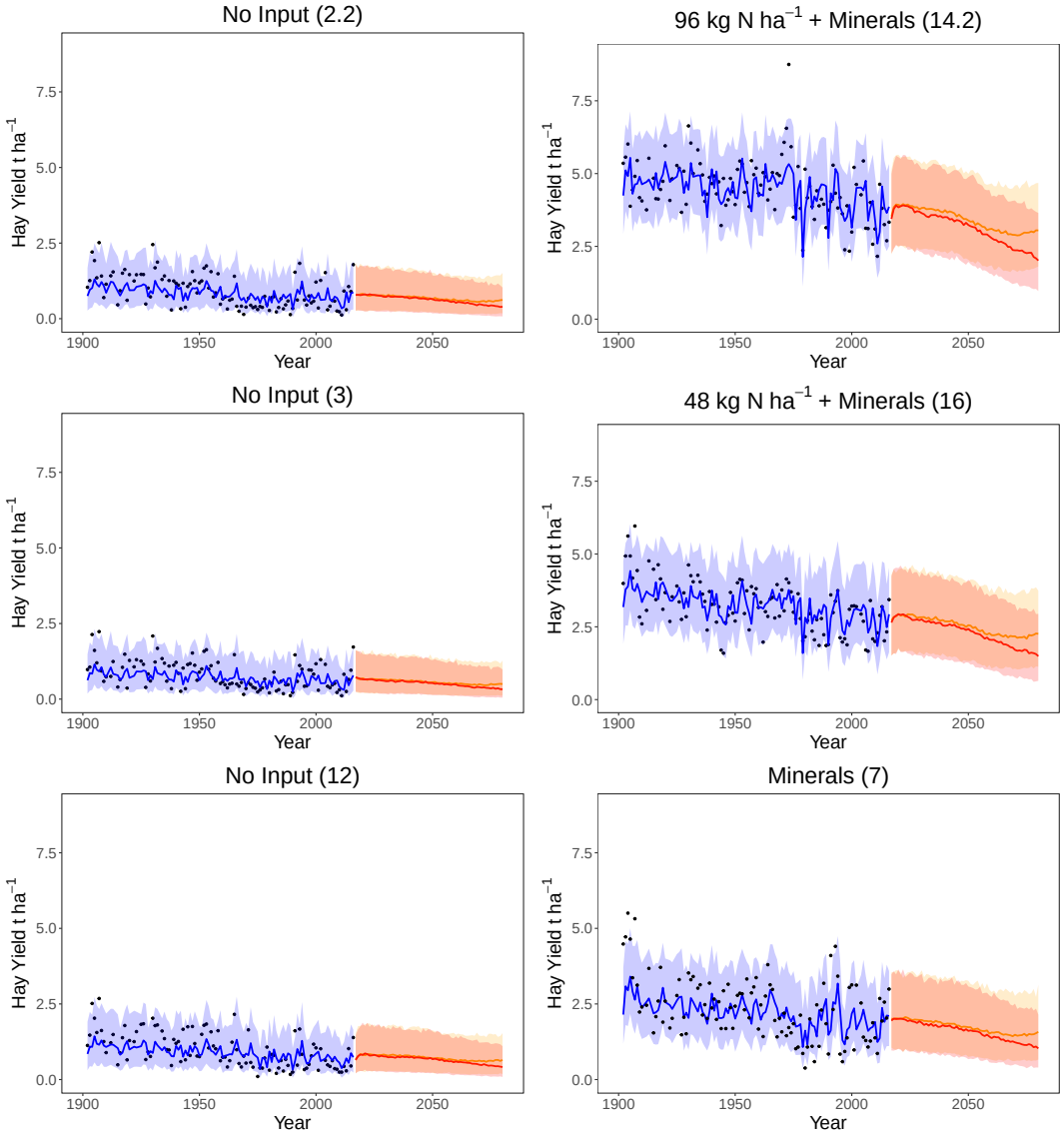

Figure 4: Fitted log-logistic mean variance relationship (Equation 1) of the Park Grass hay yield model with 89% credible interval (shaded area), with predictions of y ($\hat{y}$) on the x-axis

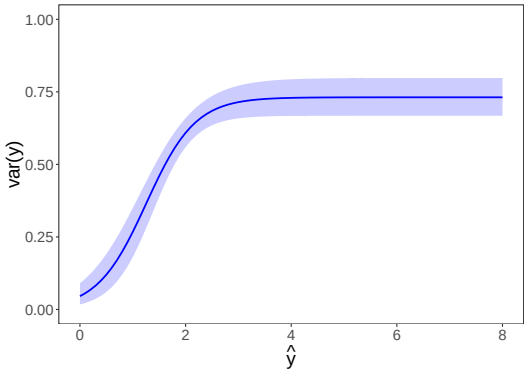

Supplementary Materials

Supplementary Table 1: Changes in spring hay yields (t ha^{-1} at 100% dry matter, with 89% credible interval) forecast for Park Grass plots 2.2, 3, 12, 14.2, 16 and 7 in 2020, 2040, 2060, and 2080 from the model given in Table 2 under GISS RCP 4.5 and 8.5 future climate scenarios. Values Δ % are the percentage change from 2020

Treatment	Year	RCP 4.5	Δ%	RCP 8.5	Δ%
No Input	2020	0.853 (0.299, 1.893)		0.868 (0.312, 1.834)	
(2.2)	2040	0.852 (0.259, 1.728)	-0.136	0.758 (0.243, 1.641)	-12.670
	2060	0.807 (0.287, 1.846)	-5.389	0.683 (0.217, 1.472)	-21.377
	2080	0.838 (0.306, 1.840)	-1.783	0.610 (0.183, 1.483)	-29.779
No Input	2020	0.702 (0.233, 1.586)		0.693 (0.220, 1.590)	
(3)	2040	0.684 (0.207, 1.568)	-2.671	0.606 (0.185, 1.429)	-12.588
	2060	0.630 (0.210, 1.543)	-10.242	0.558 (0.152, 1.326)	-19.557
	2080	0.689 (0.215, 1.644)	-1.915	0.528 (0.120, 1.339)	-23.848
No Input	2020	0.866 (0.319, 1.927)		0.867 (0.310, 1.977)	
(12)	2040	0.872 (0.330, 1.895)	0.730	0.799 (0.287, 1.758)	-7.808
	2060	0.846 (0.300, 1.838)	-2.294	0.701 (0.247, 1.582)	-19.124
	2080	0.861 (0.309, 1.846)	-0.557	0.676 (0.209, 1.484)	-22.008
96 kg N ha^{-1}	2020	4.174 (2.817, 5.817)		4.183 (2.748, 5.785)	
+ Minerals	2040	4.122 (2.678, 5.726)	-1.251	3.690 (2.245, 5.370)	-11.801
(14.2)	2060	4.065 (2.606, 5.814)	-2.625	3.363 (2.064, 4.996)	-19.607
	2080	4.229 (2.789, 6.052)	1.310	3.226 (1.927, 4.759)	-22.892
48 kg N ha^{-1}	2020	3.155 (1.814, 4.744)		3.139 (1.925, 4.705)	
+ Minerals	2040	3.076 (1.838, 4.737)	-2.528	2.764 (1.502, 4.268)	-11.949
(16)	2060	2.991 (1.827, 4.571)	-5.217	2.478 (1.260, 4.102)	-21.042
	2080	3.142 (1.917, 4.670)	-0.408	2.298 (1.142, 3.870)	-26.791
Minerals	2020	2.154 (1.095, 3.660)		2.182 (1.128, 3.688)	
(7)	2040	2.117 (1.022, 3.635)	-1.723	1.918 (0.914, 3.447)	-12.109
	2060	2.040 (0.993, 3.475)	-5.267	1.715 (0.730, 3.251)	-21.410
	2080	2.167 (1.114, 3.679)	0.607	1.618 (0.675, 3.072)	-25.832

Supplementary Figure 1: Rothamsted Meteorological Station's harvest season (Autumn to Summer) yearly summary of mean temperature (deg C) and total rainfall (mm) from 1902 to 2016 (blue), with GISS RCP 4.5 (orange) and 8.5 (red) transient future climate projections from 2017 to 2080 with 89% credible interval (shaded area)

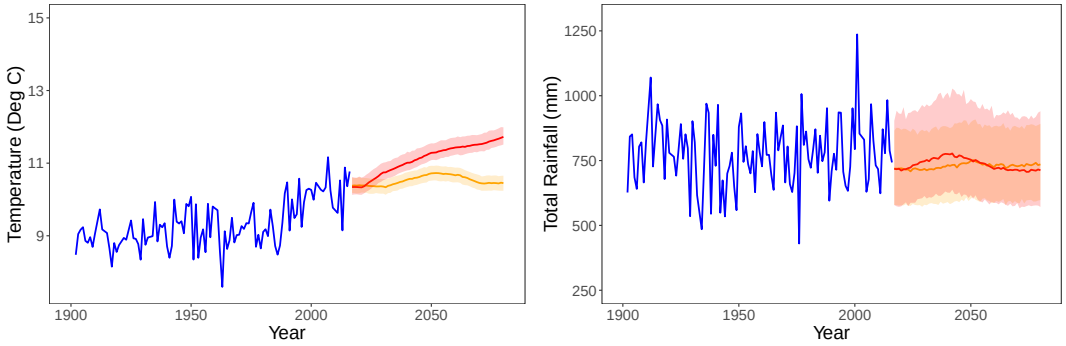

Supplementary Figure 2: The model fit (solid line) and 89% credible intervals (shaded area) of hay yields from Models 1-5 (see Table 1) of Park Grass sections 2.2, 3, 12, 14.2, 16 and 7 (•) (left panel) with corresponding mean-variance relationship (right panel)

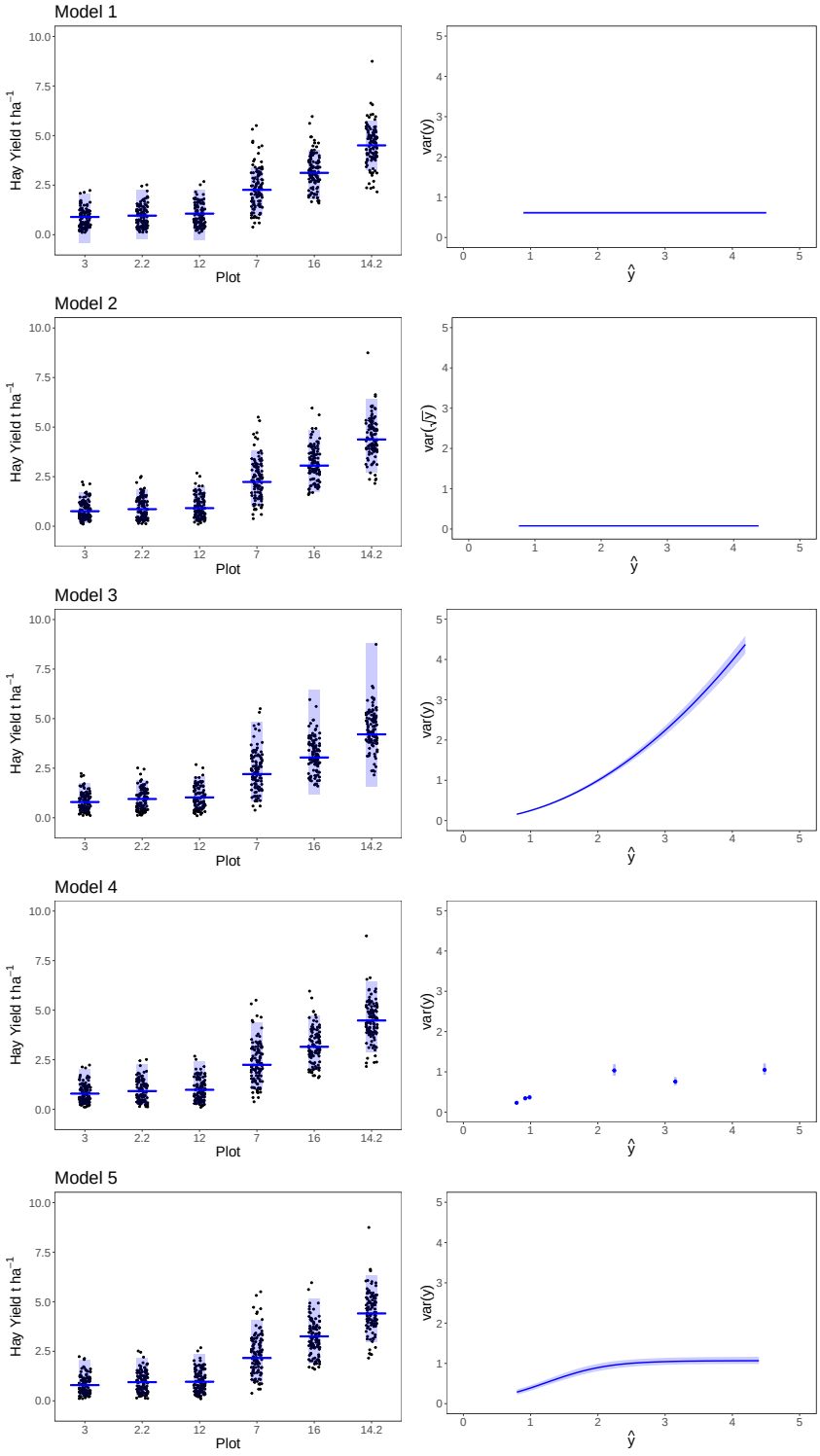

Supplementary Figure 3: Hay yields (t ha^{-1} at 100% dry matter) from Park Grass sections 2.2, 3, 12, 14.2, 16 and 7 from 1902 to 2016 (•) with forecasted hay yields from GISS RCP 4.5 (orange) and 8.5 (red) future climate scenarios. Fitted line is the posterior predictive values from the varying intercept Park Grass weather model given in Table 2 with 89% credible interval (shaded area)

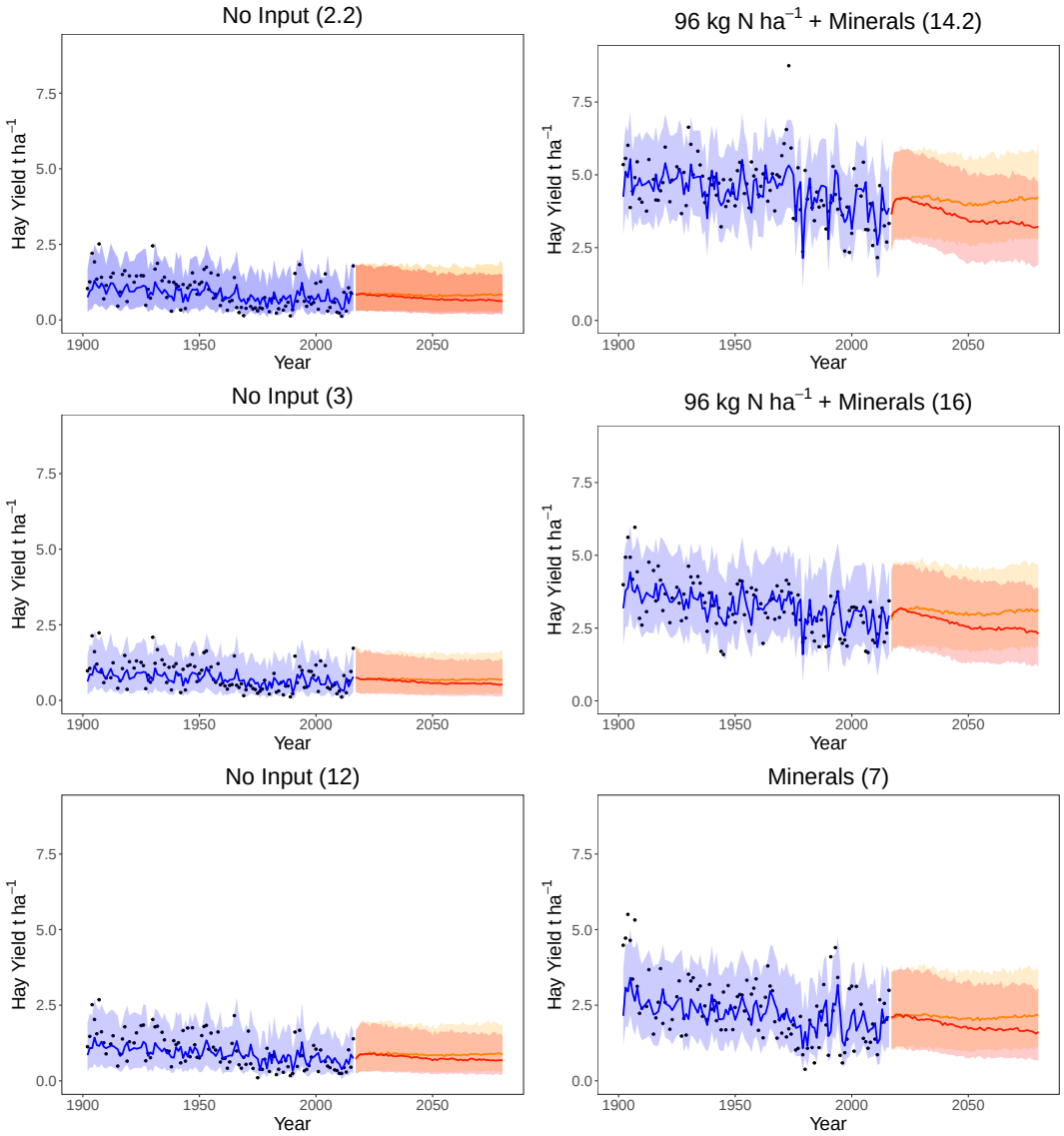

Supplementary Figure 4: The fitted relationship between hay yields (t ha^{-1} at 100% dry matter) from the varying intercept Park Grass weather model given in Table 2 for all plots 2.2, 3, 12, 14.2, 16 and 7 and autumn total rainfall (•), with 89% predictive intervals (shaded area).

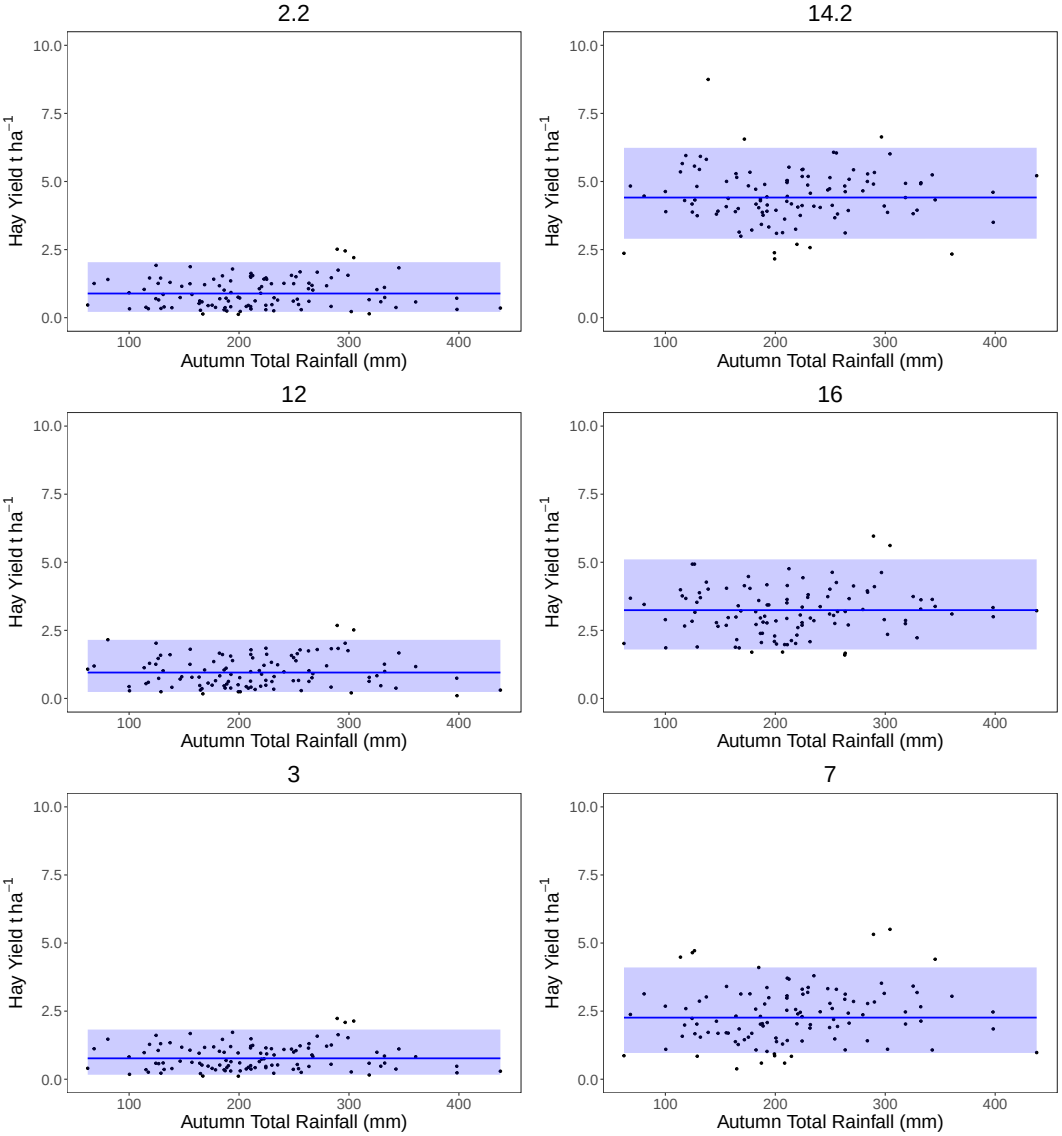

Supplementary Figure 5: The fitted relationship between hay yields (t ha^{-1} at 100% dry matter) from the varying intercept Park Grass weather model given in Table 2 for all plots 2.2, 3, 12, 14.2, 16 and 7 and winter total rainfall (•), with 89% predictive intervals (shaded area).

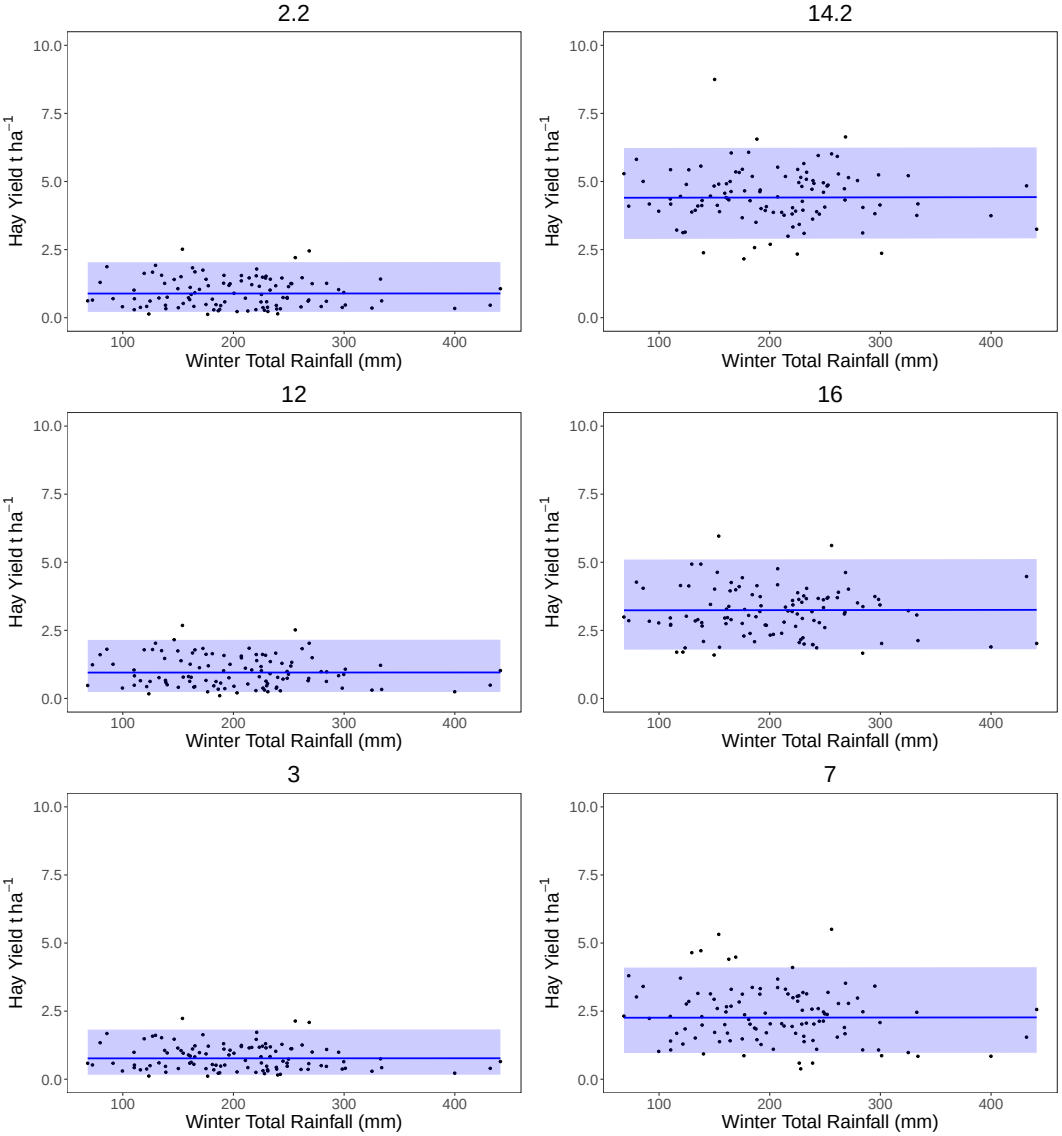

Supplementary Figure 6: The fitted relationship between hay yields (t ha^{-1} at 100% dry matter) from the varying intercept Park Grass weather model given in Table 2 for all plots 2.2, 3, 12, 14.2, 16 and 7 and spring total rainfall (•), with 89% predictive intervals (shaded area).

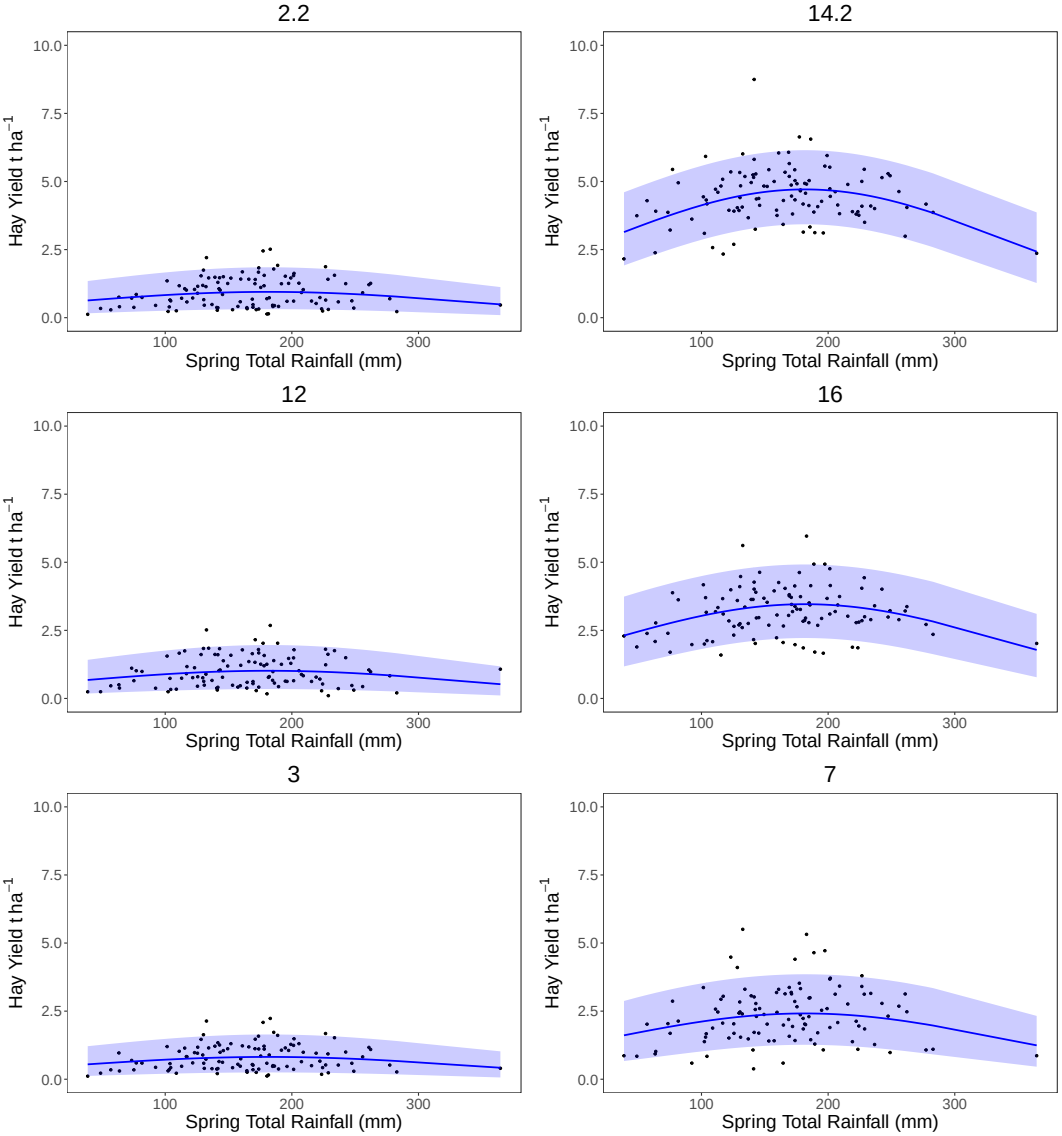

Supplementary Figure 7: The fitted relationship between hay yields (t ha^{-1} at 100% dry matter) from the varying intercept Park Grass weather model given in Table 2 for all plots 2.2, 3, 12, 14.2, 16 and 7 and mean autumn temperature (•), with 89% predictive intervals (shaded area).

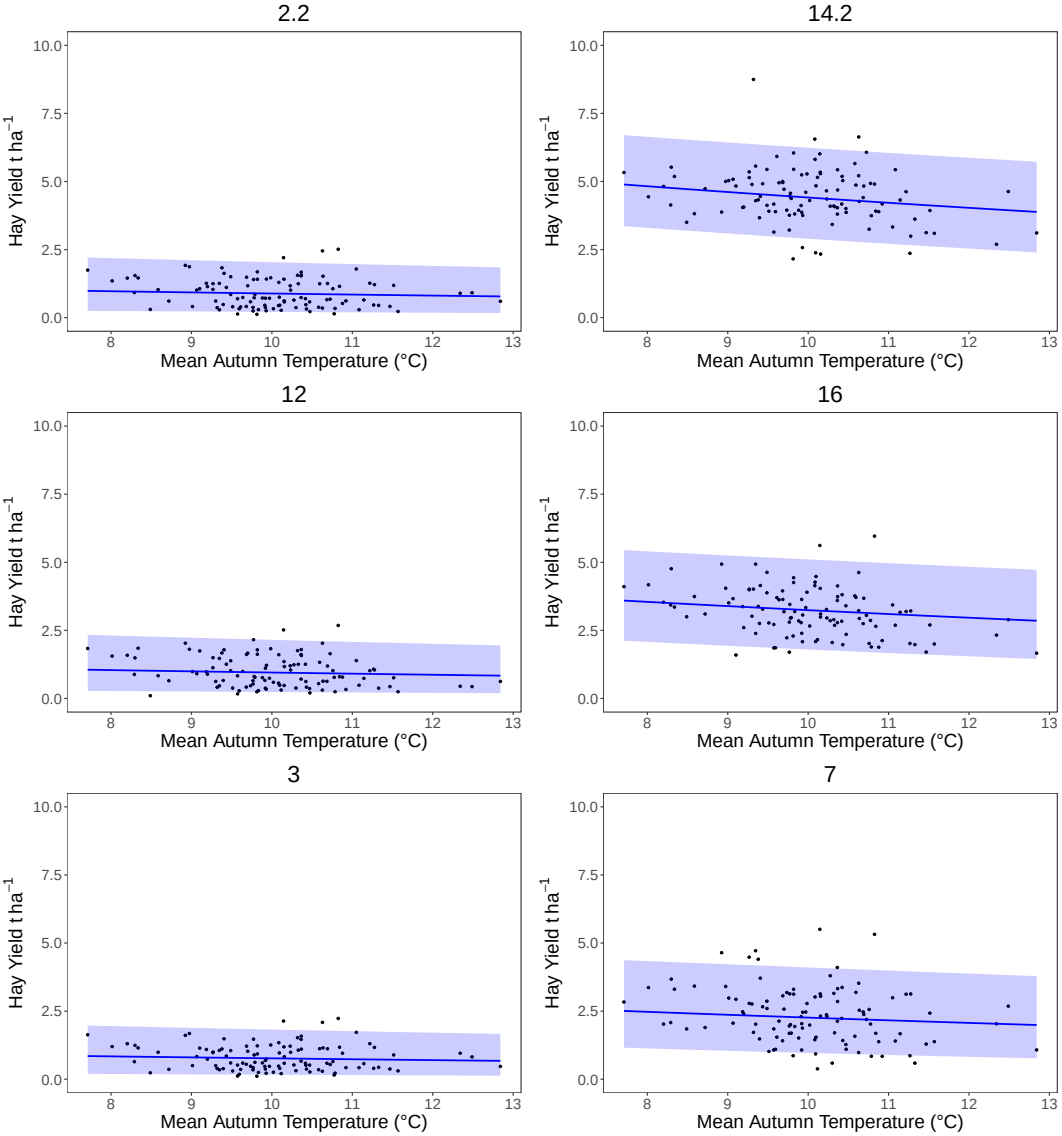

Supplementary Figure 8: The fitted relationship between hay yields (t ha^{-1} at 100% dry matter) from the varying intercept Park Grass weather model given in Table 2 for all plots 2.2, 3, 12, 14.2, 16 and 7 and mean winter temperature (•), with 89% predictive intervals (shaded area).

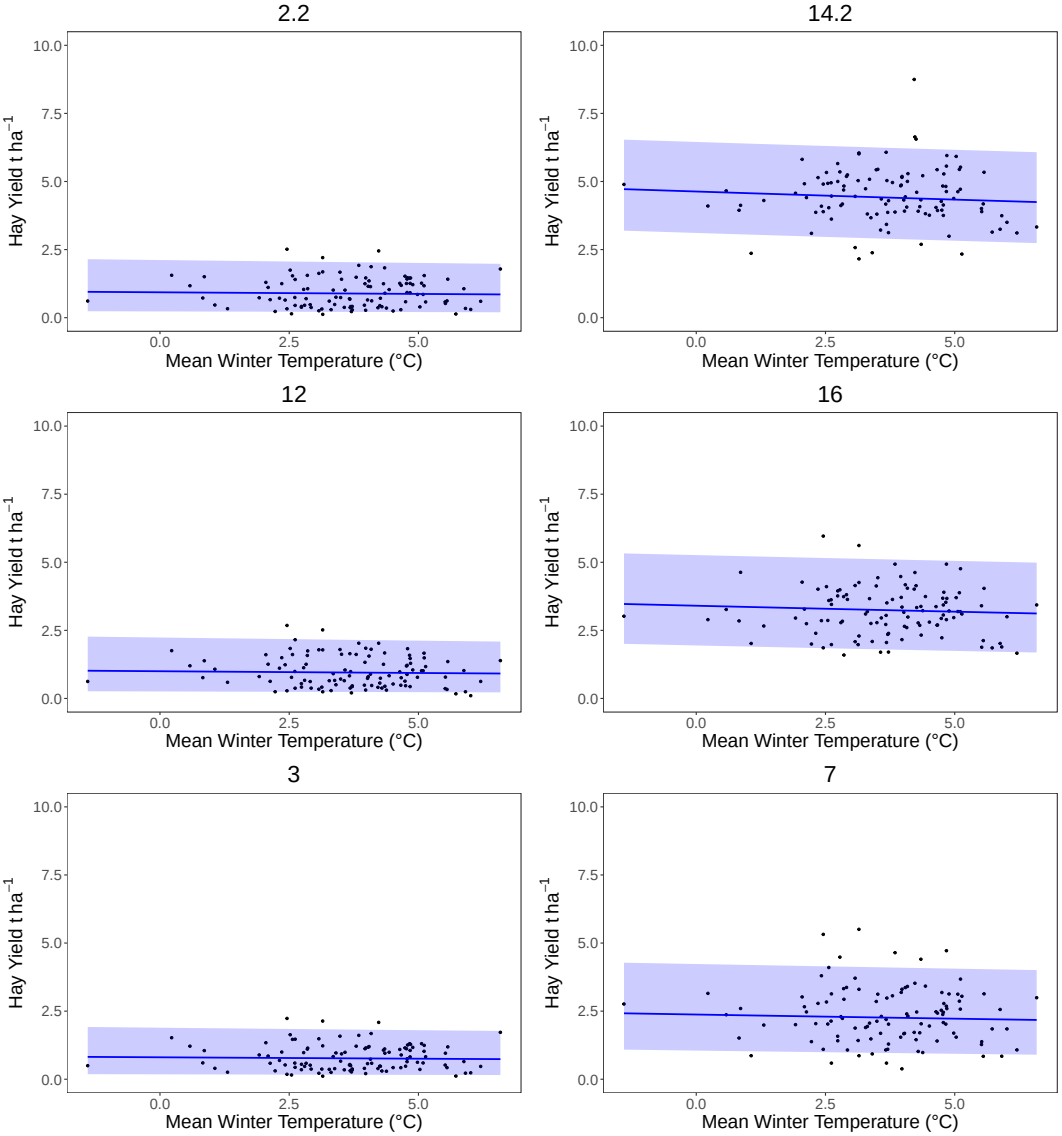

Supplementary Figure 9: The fitted relationship between hay yields (t ha^{-1} at 100% dry matter) from the varying intercept Park Grass weather model given in Table 2 for all plots 2.2, 3, 12, 14.2, 16 and 7 and mean spring temperature (•), with 89% predictive intervals (shaded area).